nature photonics

SUPPLEMENTARY INFORMATION
https://doi.org/10.1038/s41566-018-0260-y

In the format provided by the authors and unedited.

Anion-exchange red perovskite quantum dots with ammonium iodine salts for highly efficient light-emitting devices

Takayuki Chiba[1,2,3]*, Yukihiro Hayashi[1], Hinako Ebe[1], Keigo Hoshi[1], Jun Sato[1], Shugo Sato[1], Yong-Jin Pu[1,4], Satoru Ohisa[1,2,3] and Junji Kido[1,2,3]*

[1]Graduate School of Organic Materials Science, Yamagata, Japan. [2]Research Center for Organic Materials, Yamagata, Japan. [3]Frontier Center for Organic Materials, Yamagata University, Yamagata, Japan. [4]Present address: RIKEN Center for Emergent Matter Science, Saitama, Japan.
*e-mail: T-chiba@yz.yamagata-u.ac.jp; kid@yz.yamagata-u.ac.jp

Supplementary Information

Anion-exchange red perovskite quantum dots with ammonium-iodine salts for highly efficient light-emitting devices

Takayuki Chiba[1,2,3*], Yukihiro Hayashi[1], Hinako Ebe[1], Keigo Hoshi[1], Jun Sato[1], Shugo Sato[1], Yong-Jin Pu[1,4], Satoru Ohisa[1,2,3], and Junji Kido[1,2,3*]

[1]Graduate School of Organic Materials Science, [2]Research Center for Organic Materials, [3]Frontier Center for Organic Materials Yamagata University, Yamagata, Japan. [4]Pressent address: RIKEN Center for Emergent Matter Science, Saitama, Japan.

[*]Corresponding authors. E-mail: T-chiba@yz.yamagata-u.ac.jp and kid@yz.yamagata-u.ac.jp
Tel. & Fax: +81-238-26-3595

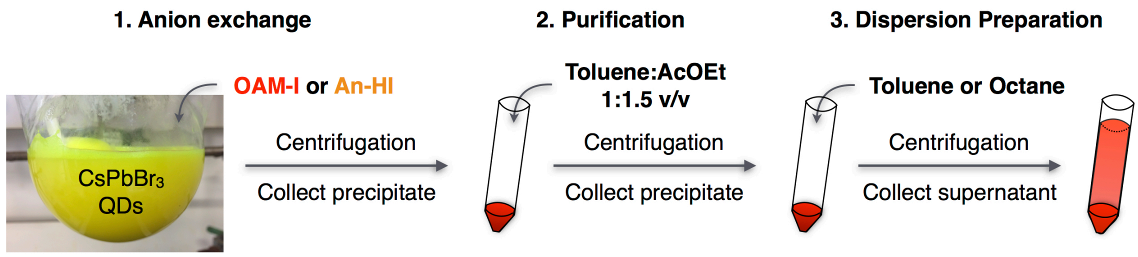

Figure S1. Scheme of anion-exchange and purification processes of perovskite QDs.

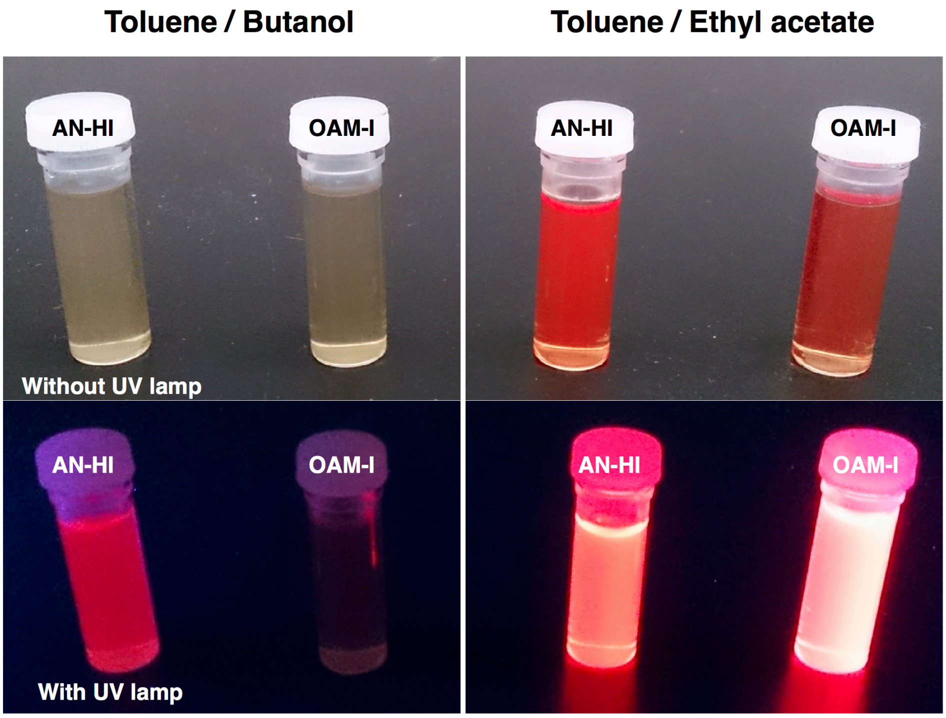

Figure S2. Images of washing solvents with different dielectric constants: butanol (ε = 17.1) and ethyl acetate (ε = 6.02). The ester solvent ethyl acetate is used as the washing solvent to remove impurities and prevent anion defects in the perovskite QDs.

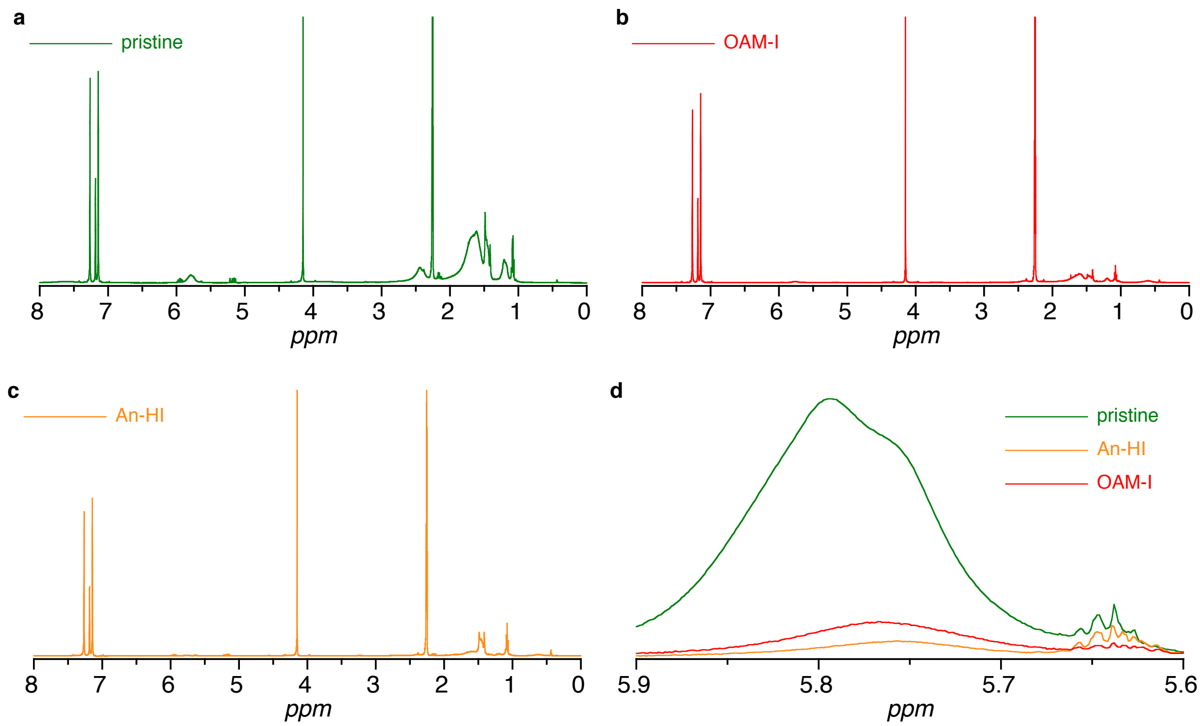

Figure S3. [1]H NMR spectra of (a) pristine $CsPbBr_3$ perovskite QDs, (b) OAM-I-based anion-exchange perovskite QDs, (c) An-HI-based anion-exchange perovskite QDs, and (d) alkene resonance signals of OA or OAM.

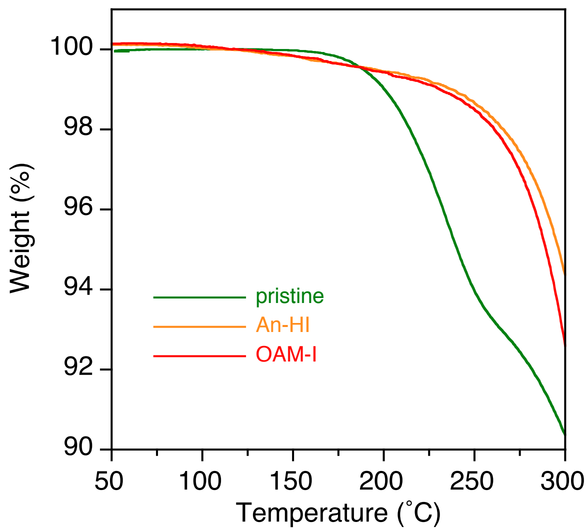

Figure S4. TGA curves of pristine $CsPbBr_3$ perovskite QDs and OAM-I-based and An-HI-based anion-exchange perovskite QDs.

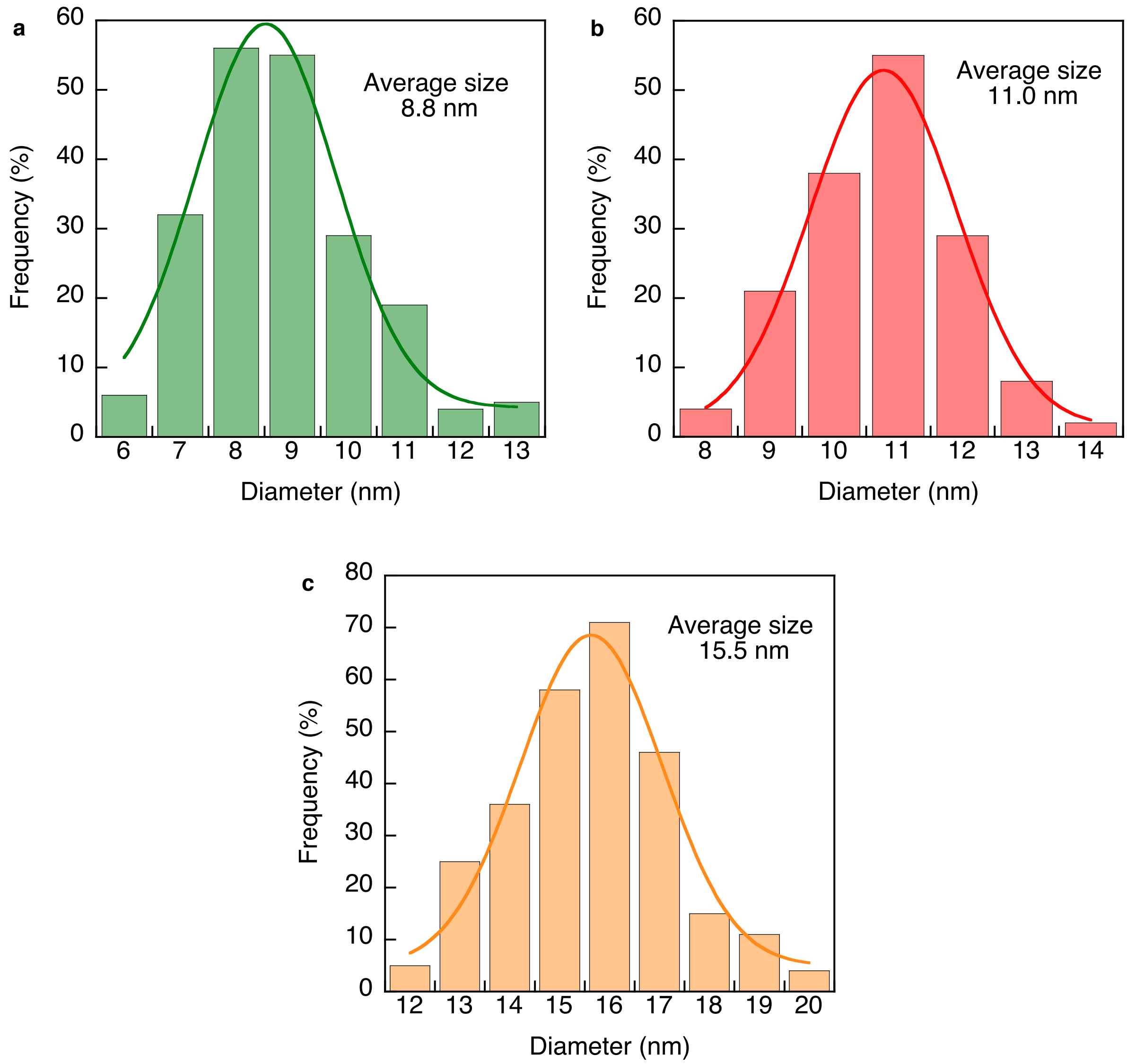

Figure S5. Size histograms of (a) pristine $CsPbBr_3$ perovskite QDs, (b) OAM-I-based anion-exchange perovskite QDs, and (c) An-HI-based anion-exchange perovskite QDs. Average size of the perovskite QDs was determined by counting more than 200 QDs from TEM images.

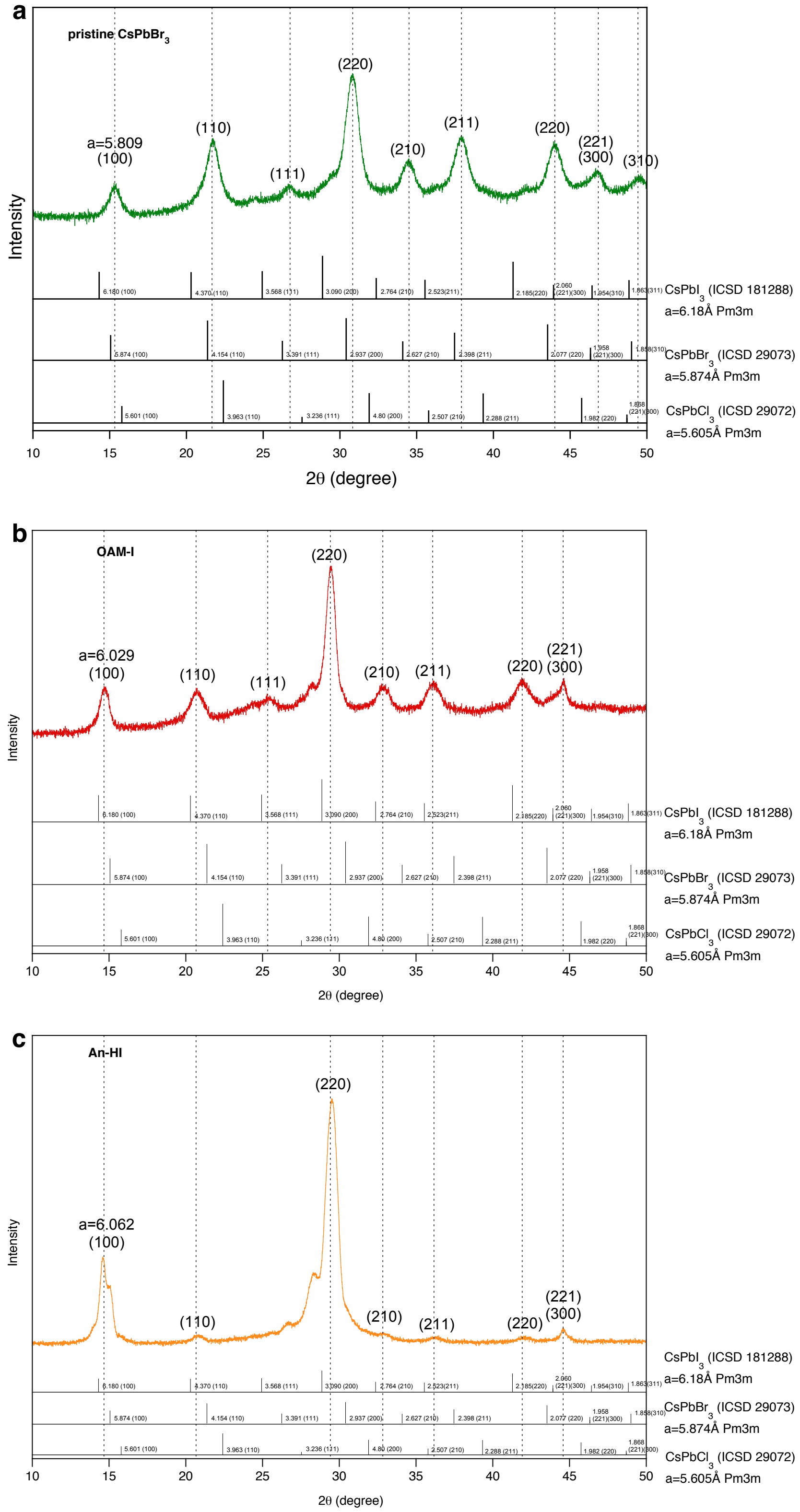

Figure S6. XRD profiles of (a) pristine $CsPbBr_3$ perovskite QDs, (b) OAM-I-based anion-exchange perovskite QDs, and (c) An-HI-based anion-exchange perovskite QDs.

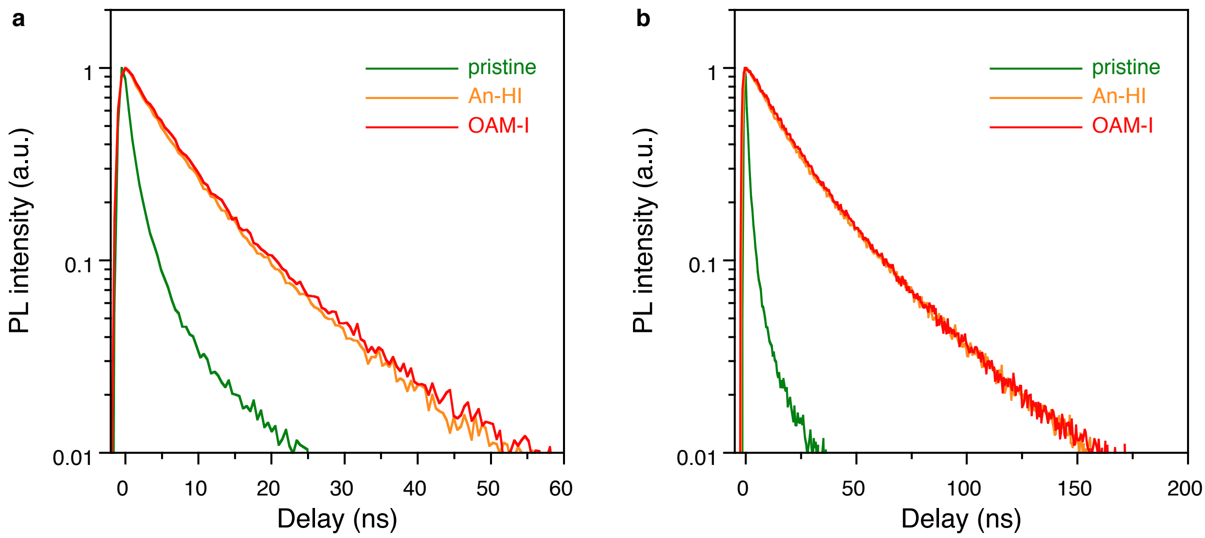

Figure S7. PL decay curves of pristine $CsPbBr_3$ perovskite QDs and OAM-I-based and An-HI-based anion-exchange perovskite QDs: (a) film and (b) solution in toluene.

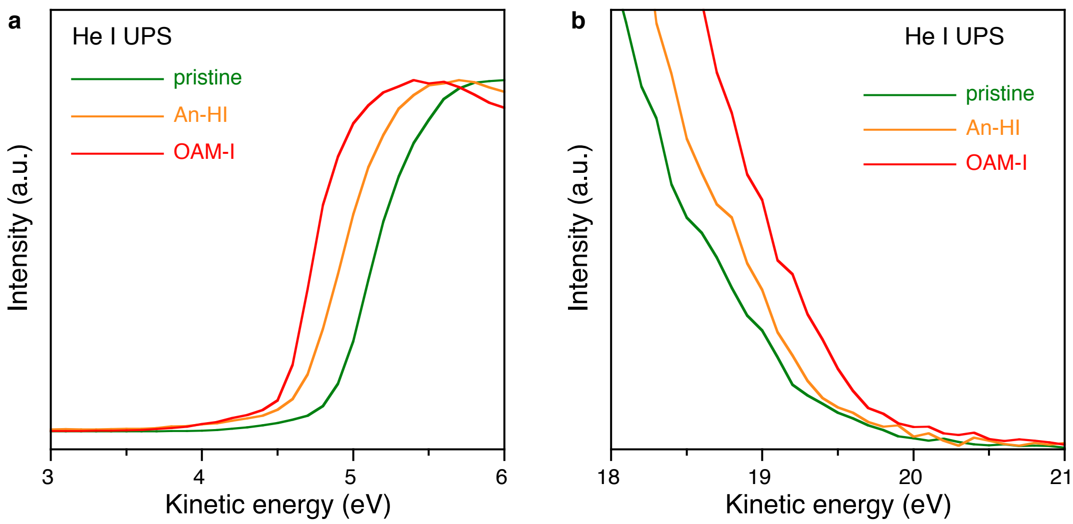

Figure S8. UPS spectra of pristine $CsPbBr_3$ perovskite QDs and OAM-I-based and An-HI-based anion-exchange perovskite QDs: (a) cut-off region and (b) band-edge region.

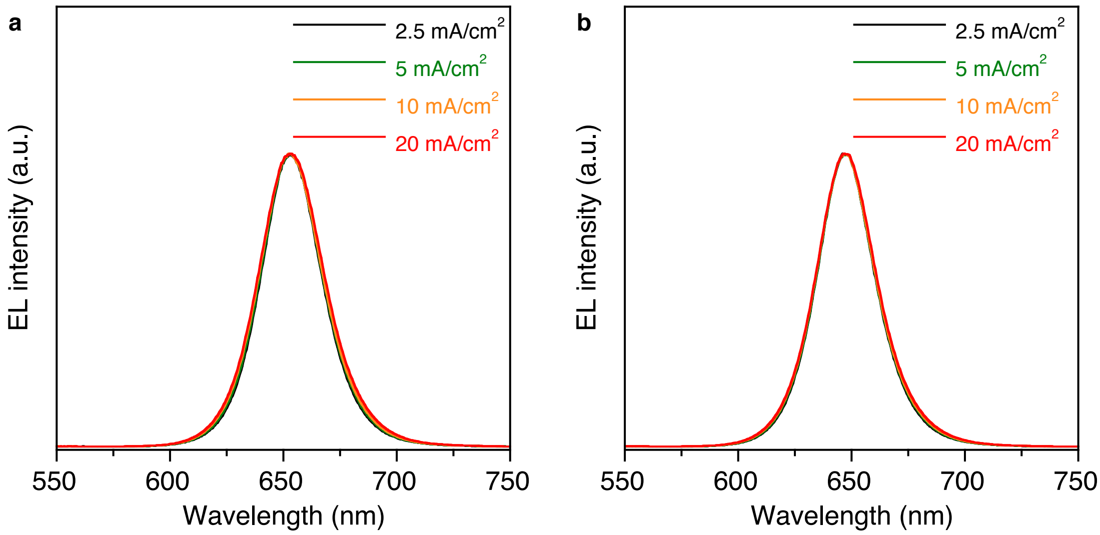

Figure S9. Current density dependence of EL spectra: (a) OAM-I-based anion-exchange perovskite QD LED and (b) An-HI-based anion-exchange perovskite QD LED. No emissions were observed from the neighboring poly-TPD and TPBi layers, indicating that the injected holes and electrons recombined at the anion-exchange red perovskite QDs.

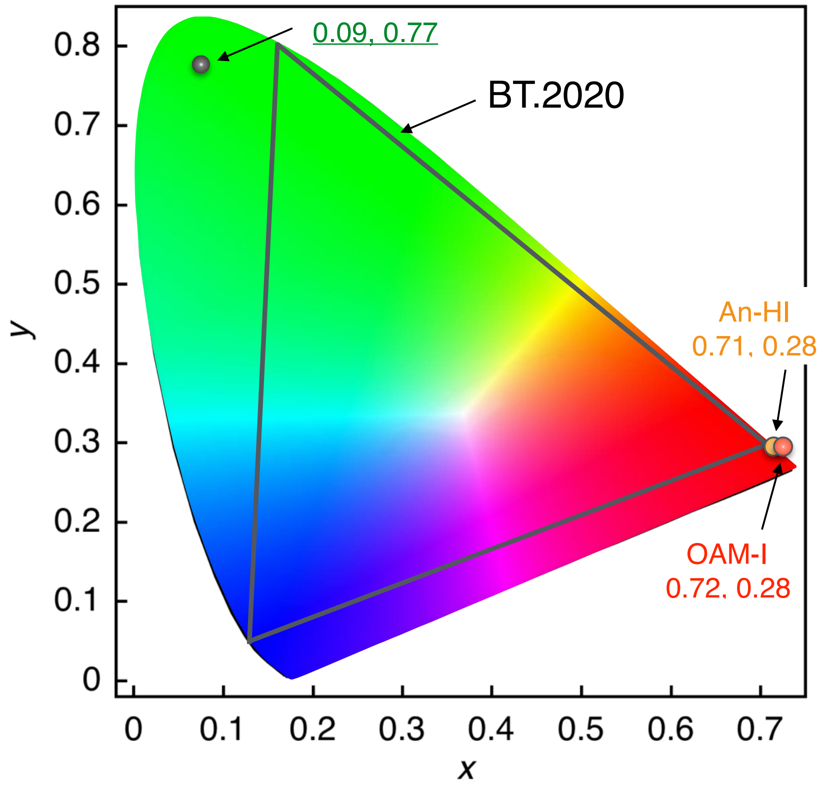

Figure S10. Commission Internationale de l'Eclairage (CIE) colour coordinates of perovskite QD LEDs. Black line indicates BT.2020 colour gamut.

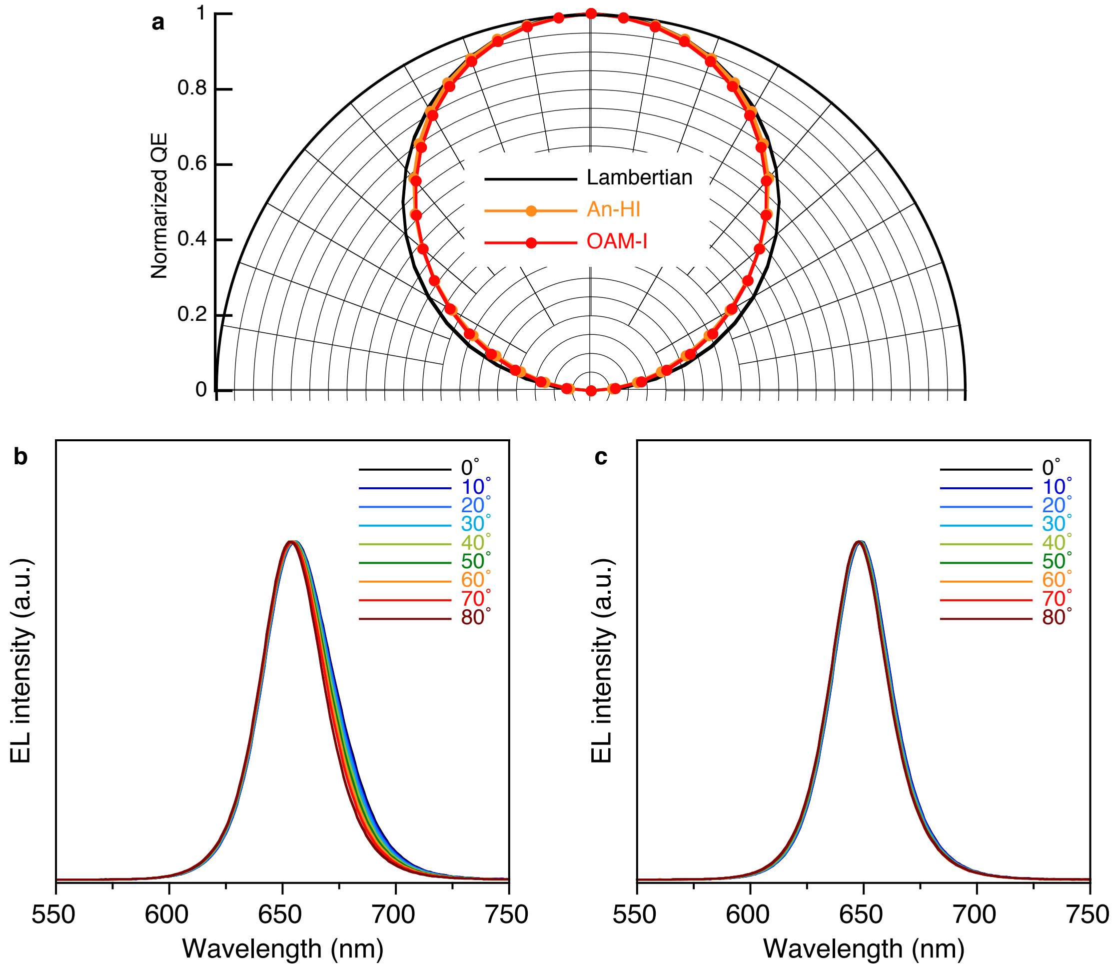

Figure S11. (a) Angular distribution of emission pattern, and EL spectra of (b) OAM-I-based anion-exchange perovskite QD LEDs and (cc) An-HI-based anion-exchange perovskite QD LEDs.

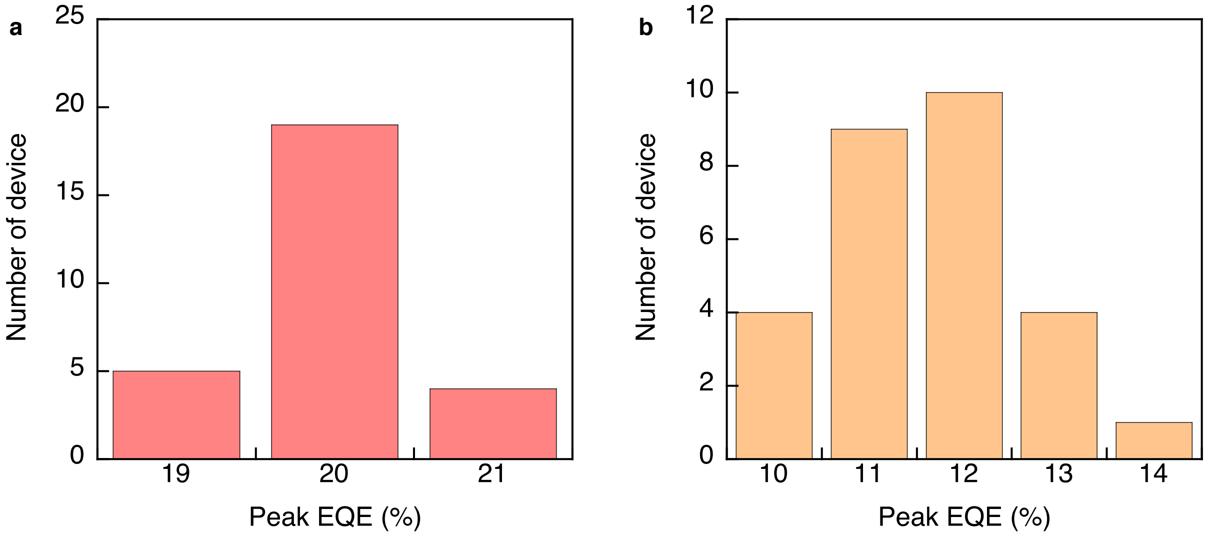

Figure S12. External quantum efficiency (EQE) histograms (28 devices) of (a) OAM-I-based anion-exchange perovskite QD LEDs and (b) An-HI-based anion-exchange perovskite QD LEDs.

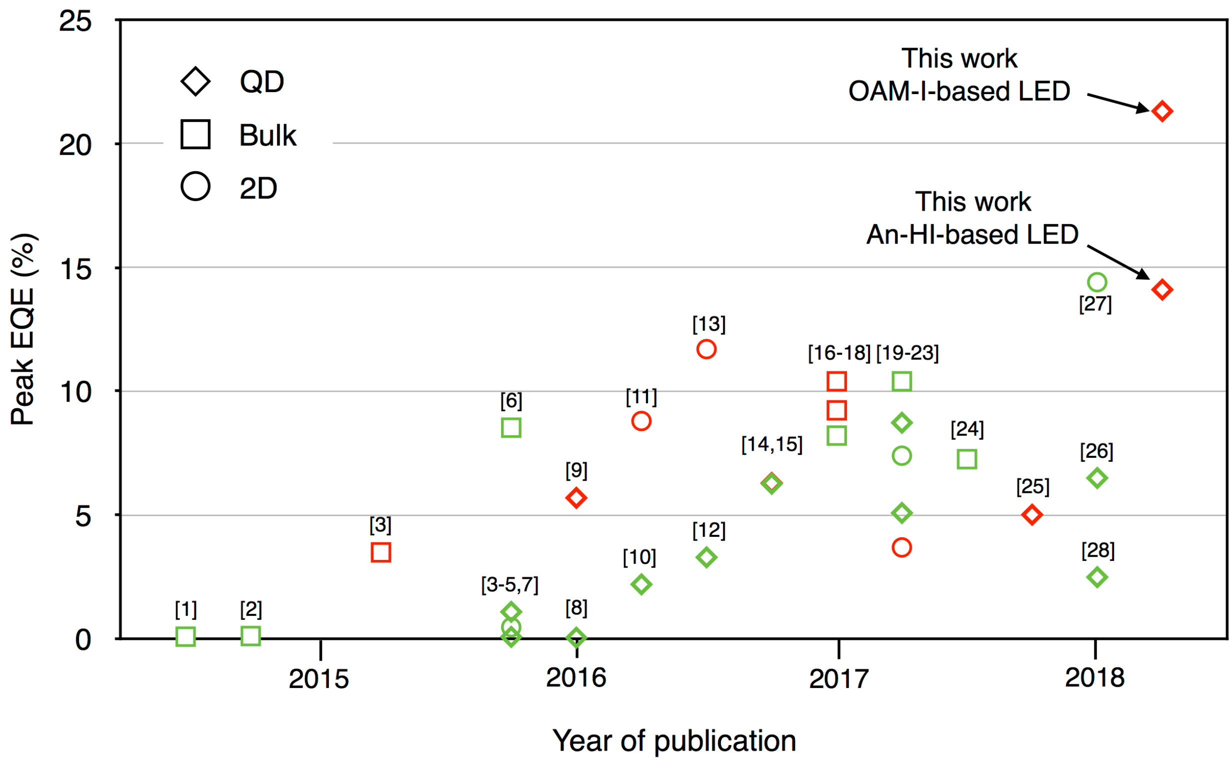

Figure S13. EQE values of recently reported perovskite-based LEDs.

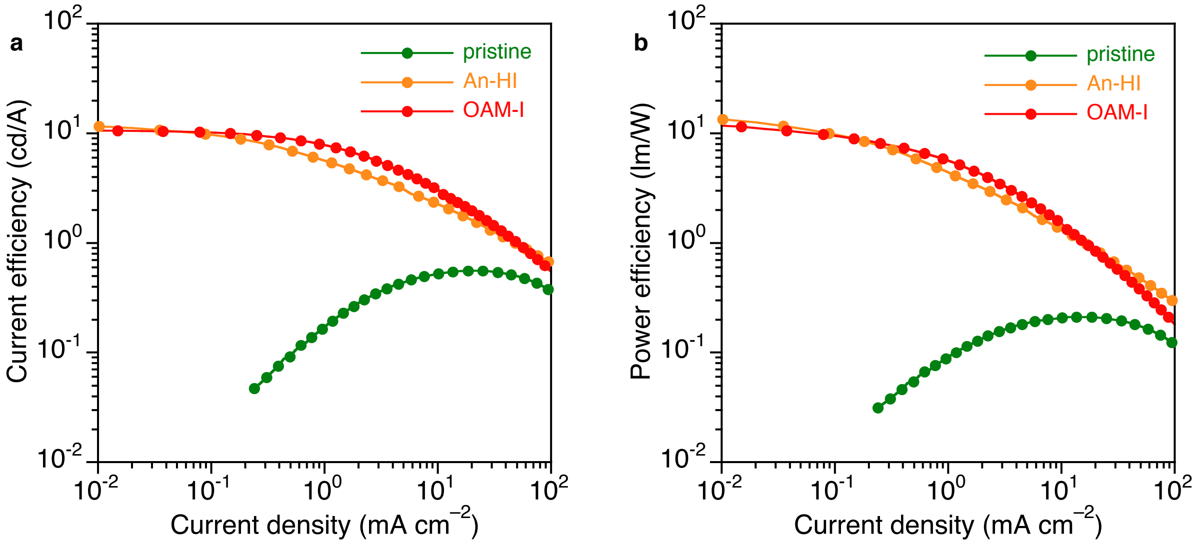

Figure S14. (a) Current efficiencies and (b) power efficiencies of pristine perovskite QD LEDs and OAM-I- and An-HI-based anion-exchange perovskite QD LEDs.

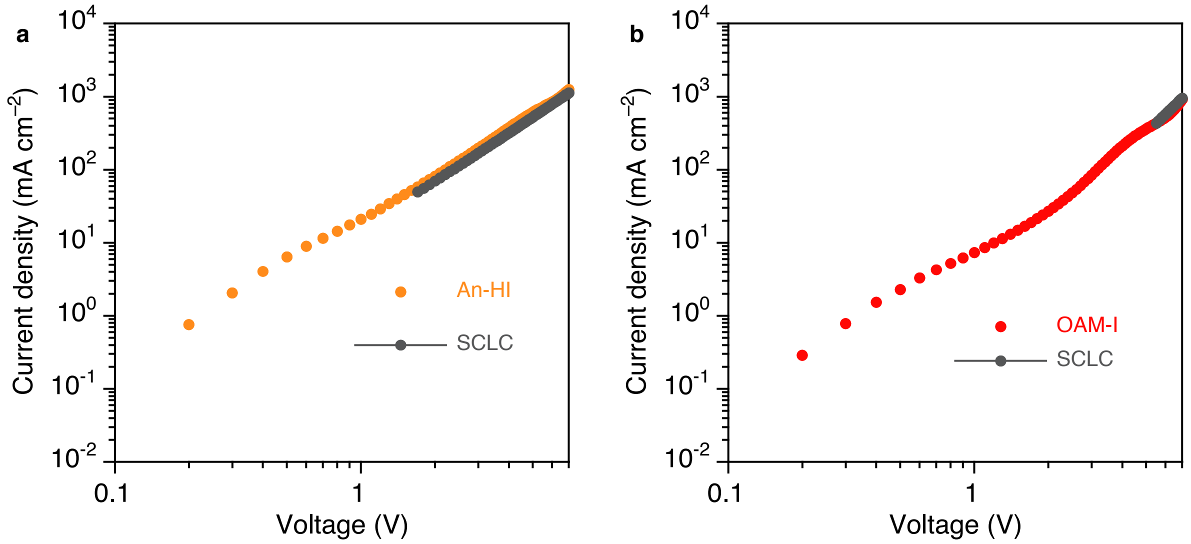

Figure S15. Current density–voltage curves and SCLC fitting of the hole-only device with (a) An-HI-based and (b) OAM-I based perovskite QD films.

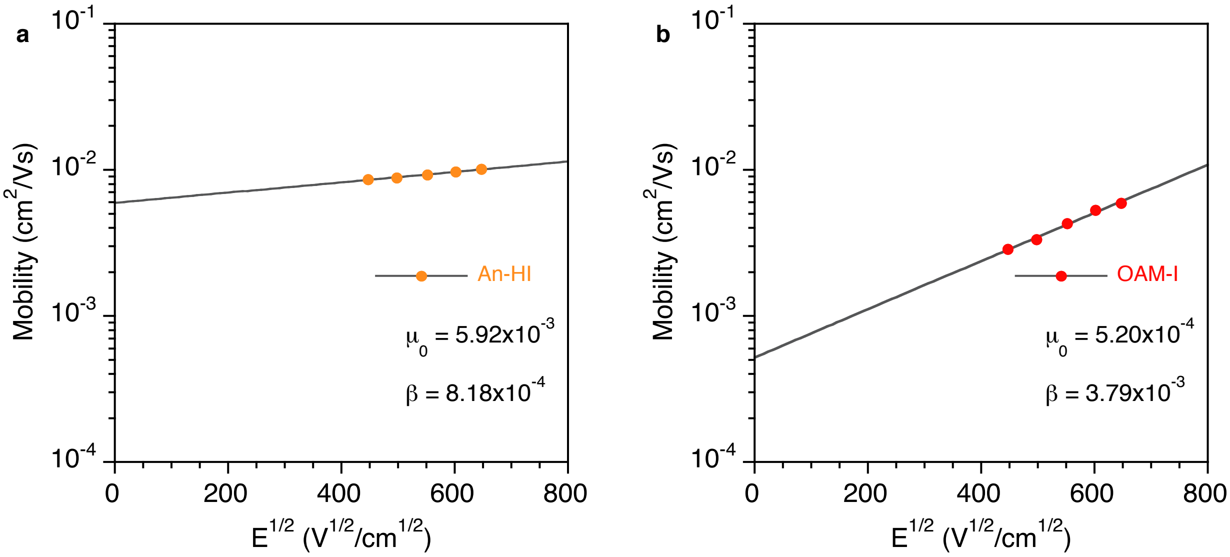

Figure S16. Calculated hole mobility at different electric fields, zero-field mobility, and field-dependent mobility.

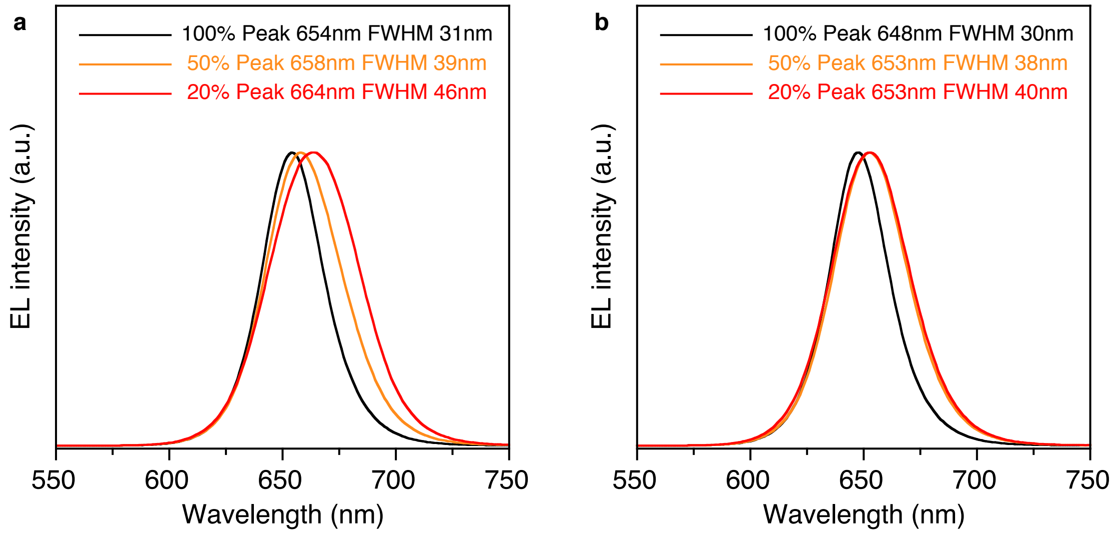

Figure S17. EL spectra during operational lifetime test at constant current density of 1.25 mA cm^{-2}: (a) OAM-I-based anion-exchange perovskite QD LEDs and (b) An-HI-based anion-exchange perovskite QD LEDs.

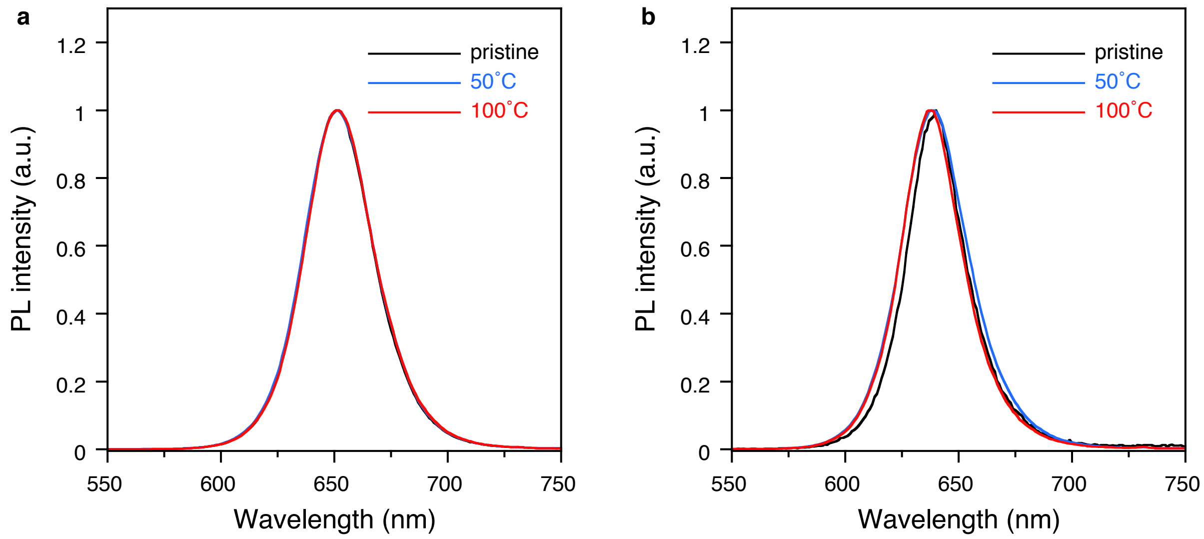

Figure S18. PL spectra of pristine (unannealed) and annealed QD samples for different annealing temperatures (50 °C and 100 °C): (a) OAM-I-based anion-exchange perovskite QD film and (b) An-HI-based anion-exchange perovskite QD film.

Table. S1 Summary of photophysical characteristics of perovskite QDs.

Sample	XPS Composition	PL peak (nm) Solution/Film	PLQY (%) Solution/Film	τ_{ave} (ns) Solution/Film	VB (eV)	CB (eV)	Eg (eV)
pristine	$CsPbBr_{2.78}$	509/510	38/15	8.2/4.7	6.1	3.7	2.38
An-HI	$CsPbBr_{0.60}I_{2.40}$	640/642	69/21	27.7/8.9	5.7	3.8	1.88
OAM-I	$CsPbBr_{0.71}I_{2.23}$	649/650	80/26	28.1/9.2	5.5	3.6	1.85

Table. S2 Performance summary of recently reported perovskite (bulk, QD, and 2D)-based LEDs

Reference	Publication date	Types	Emission layer	EL wavelength (nm)	Turn on voltage (V)	Peak EQE (%)
[1]	2014/8	Bulk	$CH_3NH_3PbBr_3$	524	3.3	0.1
[2]	2014/11	Bulk	$CH_3NH_3PbBr_3$	543	~4	0.125
[3]	2015/4	Bulk	$CH_3NH_3PbI_{3-x}Cl_x$	768	2.2	3.5
[4]	2015/10	QD	$CsPb(Br/I)_3$	586	4.6	0.09
[5]	2015/11	2D	$CH_3NH_3PbBr_3$	530	3.8	0.48
[6]	2015/12	Bulk	$CH_3NH_3PbBr_3$	540	3.2	8.53
[7]	2015/12	QD	$CH_3NH_3PbBr_3$	521	2.9	1.1
[8]	2016/1	QD	$CsPbBr_3$	516	3.5	0.06
[9]	2016/3	QD	$CsPbI_3$ with OA,OAm,TMA	698	2.2	5.7
[10]	2016/4	QD	$CsPbBr_3$- $CsPb_2Br_5$	527	4.6	2.21
[11]	2016/6	2D	$PEA_2MA_{n-1}Pb_nBr_{3n+1}$	~760	4	8.8
[12]	2016/8	QD	$CsPbBr_3$-DDAB	515	3.0	3.0
[13]	2016/9	2D	$NMA_2FAPb_2I_6Br$	685	1.3	11.7
[14]	2016/10	QD	$CsPb(Br/I)_3$	648	1.9	6.3
[15]	2016/11	QD	$CsPbBr_3$	512	3.4	6.27
[16]	2017/1	Bulk	$BAI:MAPbI_3$	748	3	10.4
[17]	2017/2	Bulk	$Cs_{10}(MA_{0.17}FA_{0.88})_{(100-x)}PbBr_{0.33}I_{2.67}$	750	2.8	9.23
[18]	2017/3	Bulk	$MAPbBr_3$	~538	-	8.21
[19]	2017/4	2D	$NCPI_6Cl$	688	2.0	3.7
[20]	2017/5	QD	$CsPbBr_3$	512	2.7	8.73
[21]	2017/5	2D	$PEA_2(MA)_{n-1}Pb_nI_{3n+1}$	526	-	7.4
[22]	2017/6	QD	$CH_3NH_3PbBr_3$	~520	3.3	5.09
[23]	2017/6	Bulk	$Cs_{0.87}MA_{0.13}PbBr_3$	520	2.9	10.4
[24]	2017/9	Bulk	$MAPbBr_3$	529	-	7.26
[25]	2017/12	QD	$CsPbI_3$	688	4.5	5.02
[26]	2018/1	QD	$CsPbBr_3$	516	2.8	6.5
[27]	2018/2	2D	$PEA_2(FAPbBr_3)_{n-1}PbBr_4$	532	-	14.4
[28]	2018/2	QD	$CsPbBr_3$	516	-	2.5
This work		QD	$CsPb(Br/I)_3$ with An-HI	645	2.6	14.1
This work		QD	$CsPb(Br/I)_3$ with OAM-I	653	2.8	21.3

Table. S3 Summary of perovskite QD LED characteristics.

Device	Peak EL (nm)	V (V) 1/100 cd m^{-2}	PE (lm W^{-1}) 100 cd m^{-2}/peak	CE (cd A^{-1}) 100 cd m^{-2}/peak	EQE (%) 100 cd m^{-2}/peak	Lambertian factor
pristine	511	4.3/6.2	0.44/0.44	0.87/0.89	0.55/0.56	--
An-HI	645	2.7/4.5	2.8/12.9	4.2/11.6	5.1/14.1	0.91
OAM-I	653	2.8/4.6	4.9/11.6	7.3/10.6	14.6/21.3	0.92

Reference

1. Tan, Z. K. *et al*. Bright light-emitting diodes based on organometal halide perovskite. *Nat. Nanotechnol.* **9**, 687-692 (2014).
2. Kim, Y. H. *et al*. Multicolored organic/inorganic hybrid perovskite light-emitting diodes. *Adv. Mater.* **27**, 1248-1254 (2015).
3. Wang, J. *et al*. Interfacial control toward efficient and low-voltage perovskite light-emitting diodes. *Adv. Mater.* **27**, 2311-2316 (2015).
4. Song, J. *et al*. Quantum Dot Light-Emitting Diodes Based on Inorganic Perovskite Cesium Lead Halides (CsPbX3). *Adv. Mater.* **27**, 7162-7167 (2015).
5. Ling, Y. C. *et al*. Bright Light-Emitting Diodes Based on Organometal Halide Perovskite Nanoplatelets. *Adv. Mater.* **28**, 305-311 (2016).
6. Cho, H. *et al*. Overcoming the electroluminescence efficiency limitations of perovskite light-emitting diodes. *Science* **350**, 1222-1225 (2015).
7. Huang, H. L. *et al*. Emulsion Synthesis of Size-Tunable CH3NH3PbBr3 Quantum Dots: An Alternative Route toward Efficient Light-Emitting Diodes. *ACS Appl. Mater. Interfaces.* **7**, 28128-28133 (2015).
8. Zhang, X. *et al*. Enhancing the Brightness of Cesium Lead Halide Perovskite Nanocrystal Based Green Light-Emitting Devices through the Interface Engineering with Perfluorinated Ionomer. *Nano Lett.* **16**, 1415-1420 (2016).
9. Li, G. *et al*. Highly Efficient Perovskite Nanocrystal Light-Emitting Diodes Enabled by a Universal Crosslinking Method. *Adv. Mater.* **28**, 3528-3534 (2016).
10. Zhang, X. L. *et al*. All-Inorganic Perovskite Nanocrystals for High-Efficiency Light Emitting Diodes: Dual-Phase CsPbBr3-CsPb2Br5 Composites. *Adv. Funct. Mater.* **26**, 4595-4600 (2016).
11. Yuan, M. J. *et al*. Perovskite energy funnels for efficient light-emitting diodes. *Nat. Nanotechnol.* **11**, 872-877 (2016).
12. Pan, J. *et al*. Highly Efficient Perovskite-Quantum-Dot Light-Emitting Diodes by Surface Engineering. *Adv. Mater.* **28**, 8718-8725 (2016).
13. Wang, N. N. *et al*. Perovskite light-emitting diodes based on solution-processed self-organized multiple quantum wells. *Nat. Photon.* **10**, 699-704 (2016).
14. Zhang, X. *et al*. Bright Perovskite Nanocrystal Films for Efficient Light-Emitting Devices. *J. Phys. Chem. Lett.* **7**, 4602-4610 (2016).
15. Li, J. *et al*. 50-Fold EQE Improvement up to 6.27% of Solution-Processed All-Inorganic Perovskite CsPbBr3 QLEDs via Surface Ligand Density Control. *Adv. Mater.* **29**, 1603885 (2017).

16. Xiao, Z. *et al*. Efficient perovskite light-emitting diodes featuring nanometre-sized crystallites. *Nat. Photon*. **11**, 108-115 (2017).
17. Kim, H. P. *et al*. High-Efficiency, Blue, Green, and Near-Infrared Light-Emitting Diodes Based on Triple Cation Perovskite. *Adv. Opt. Mater*. **5**, 1600920 (2017).
18. Lee, J. W. *et al*. In-Situ Formed Type I Nanocrystalline Perovskite Film for Highly Efficient Light-Emitting Diode. *ACS Nano* **11**, 3311-3319 (2017).
19. Zhang, S. T. *et al*. Efficient Red Perovskite Light-Emitting Diodes Based on Solution-Processed Multiple Quantum Wells. *Adv. Mater*. **29**, 1606600 (2017).
20. Chiba, T. *et al*. High-Efficiency Perovskite Quantum-Dot Light-Emitting Devices by Effective Washing Process and Interfacial Energy Level Alignment. *ACS Appl. Mater. Interfaces*. **9**, 18054-18060 (2017).
21. Quan, L. N. *et al*. Tailoring the Energy Landscape in Quasi-2D Halide Perovskites Enables Efficient Green-Light Emission. *Nano Lett*. **17**, 3701-3709 (2017).
22. Kim, Y. H. *et al*. Highly Efficient Light-Emitting Diodes of Colloidal Metal-Halide Perovskite Nanocrystals beyond Quantum Size. *ACS Nano* **11**, 6586-6593 (2017).
23. Zhang, L. Q. *et al*. Ultra-bright and highly efficient inorganic based perovskite light-emitting diodes. *Nat. Commun*. **8**, 15640 (2017).
24. Peng, X. F. *et al*. Modified Conducting Polymer Hole Injection Layer for High-Efficiency Perovskite Light-Emitting Devices: Enhanced Hole Injection and Reduced Luminescence Quenching. *J. Phys. Chem. Lett*. **8**, 4691-4697 (2017).
25. Pan, J. *et al*. Bidentate Ligand-Passivated CsPbI3 Perovskite Nanocrystals for Stable Near-Unity Photoluminescence Quantum Yield and Efficient Red Light-Emitting Diodes. *J. Am. Chem. Soc*. **140**, 562-565 (2018).
26. Tan, Y. S. *et al*. Highly Luminescent and Stable Perovskite Nanocrystals with Octylphosphonic Acid as a Ligand for Efficient Light-Emitting Diodes. *ACS Appl. Mater. Interfaces*. **10**, 3784-3792 (2018).
27. Yang, X. L. *et al*. Efficient green light-emitting diodes based on quasi-two-dimensional composition and phase engineered perovskite with surface passivation *Nat. Commun*. **9**, 570 (2018).
28. Krieg, F. *et al*. Colloidal CsPbX3 (X = CI, Br, I) Nanocrystals 2.0: Zwitterionic Capping Ligands for Improved Durability and Stability. *ACS Energy Lett*. **3**, 641-646 (2018).